International Symposium of Research Students on Material Science and Engineering
December 20-22, 2004, Chennai, India
Department of Metallurgical and Materials Engineering, Indian Institute of Technology Madras

STUDIES ON PHOSPHORIC IRONS FOR CONCRETE REINFORCEMENT APPLICATIONS

Sahoo Gadadhar and R. Balasubramaniam
Department of Materials and Metallurgical Engineering
Indian Institute of Technology, Kanpur 208 016, INDIA

ABSTRACT

The possible use of phosphoric irons for concrete reinforcing applications has been addresed. Three phosphoric irons (Fe-0.11P-0.028C, Fe-0.32P-0.028C and Fe-0.49P-0.028C, wt.%) were ingot melted and forged between 1050^0C and 1100^0C in the dual phase region to avoid grain boundary embrittlement. The mechanical properties of the phosphoric irons were comparable with that of commercial steel bar. Potentiodynamic polarization and electrochemical spectroscopy (EIS) studies in simulated. pore solution (saturated calcium hydroxide of pH 12.5) containing chloride ions indicated that the threshold chloride content for passive film breakdown were higher for phosphoric irons. The improved corrosion resistance of phosphoric irons has been understood based on presence of phosphorus in solid solution.

Key words: Phosphoric iron; concerete reinforcement; mechanical behavior; potentiodynamic polarization; electrochemical impedance spectroscopy.

1. INTRODUCTION

Corrosion of concrete reinforcing steel is of great concern because it is probably the most widespread cause of degradation of reinforced concrete structures. It has been estimated that the annual direct cost of bridge infrastructure corrosion to the U.S. economy is $8.3 billion, with indirect costs approximately 10 times higher [1]. Initially, the reinforcing steel embedded in concrete is naturally protected by passivation due to the high alkalinity of the pore solution (pH 13.5) [2,3]. However, the passive surface film can be destroyed by aggressive ions like chlorides. These ions may have been present in the concrete constituents right from the beginning. They can also be introduced into the concrete through ingress during the service life. Acidification of the environment near the rebar (carbonation) also results in loss of passivity [2]. In chloride-containing environments, the initiation of corrosion occurs only when the chloride content is higher than a threshold value [4]. This value, calculated per cement mass or as ratio of chlorides to hydroxides, has been taken as a constant value by many authors [4-6]. Therefore, the effect of chloride ion on passive film breakdown is of great importance to ferrous alloy used for concrete reinforcement application. There are several methods suggested to minimize the corrosion of rebars [1,7] like epoxy-coated rebar, coating on concrete, corrosion inhibitor addition to cement to maintain passivity, cathodic protection using conductive coating anodes, use of stainless steel rebar, high-performance concrete and metalizing surface coatings. Each method has its own limitation and scope for large-scale application is limited [7]. It will be worthwhile designing a cheap ferrous alloy that would withstand corrosion in the concrete environment and at the same time possess the required mechanical properties. In this context it is interesting to note the relatively good corrosion resistance of phosphorus-containing iron [8-12]. This provided the impetus to study the possible use of phosphoric iron for concrete reinforcement application.

Optimum strength and ductility are important requirements for reinforcement bar. The necessary strength can be obtained in phosphoric irons because P is a good solid solution strengthening element in iron [13, 14]. The presence of P also promotes marked work hardening. However, P promotes cold shortness or brittleness during cold working due to segregation to grain boundaries [15-17]. Due to this deleterious effect, concentration of P is maintained less than 0.05 % in modern steel making [18]. The deleterious effect of P on ductility can be minimized by maintaining a low amount of carbon, preferably at the grain boundaries and by appropriate heat treatments [14, 20, 21]. The aim of the present study is to evaluate phosphoric irons for possible concrete reinforcement application.

2. EXPERIMENTAL

Three pencil ingots (80 cm long and 100 cm^2 cross section) of Fe-C-P alloys of different compositions were prepared in a 200 kg capacity induction melting furnace (at Chandel Engineering Works, Kanpur) in air by the addition of a ferro-phosphorus alloy to the soft iron, which possessed similar impurities like in mild steel. Some steel scraps were also added to balance the carbon concentration. Unlike the earlier studies on phosphorous-containing irons [20, 21], the use of electrolytic iron and vaccum melting was deliberately avoided because one of the aims of the study was to simulate actual melting practice in industrial scale. The ingots were named as sample A (Fe-0.11P-0.028C), sample B (Fe-0.32P-0.028C) and sample C (Fe-0.49P-0.028C). All the composition mentioned in this paper are in wt. %. The compositions were determined using spectral analysis method and the impurities were comparable to that observed in mild steel used for concrete reinforcement applications. It must be noted that carbon was not avoided by deliberately kept at a low value. As carbon is an interstitial solute and P a substitutional solid solute, they will avoid each other. In case carbon can be segregated to the grain boudaries, it will further result in minimizing P segregation to the grain boudaries.

The cast ingots were cut into smaller sizes and these pieces were provided a homogenization treatment by soaking at 1100^0C for four hours. They were then forged into 16mm to 25mm dia. bars in the temperature range 1050^0C to 1100^0C at the Field Gun Factory, Kanpur. Based on the Fe-P phase diagram [22], which reveals a gamma loop at high temperature, the temperature range of 1050^0C-1100^0C corresponds to the dual phase (ferrite and austenite) region in the case of sample B and C, while the sample A was in the fully austenitic state during forging. The purpose behind heat treating phosphoric iron in the dual phase region has been explained in detail elsewhere [11]. The basic philosophy was to precipitate austenite along the grain boundaries which results in lower P content at these region due to the lower solubility of P in austenite. On cooling down, this inhomogeneous P distribution remains. This is anticipated to improve ductility because P would be avoided at grain boundary locations. The microstructures of the forged samples were understood using Oberhoffer and 3% nital as etchants. The usefulness of using the Oberhoffer etchant (500ml H_2O + 30 g $FeCl_3$ + 0.5 g $SnCl_2$ + 1 g $CuCl_2$ + 500 ml C_2H_5OH + 50 ml HNO_3) to reveal phosphorus compositional inhomogenities has been explained elsewhere [23]. In order to compare the properties of the phosphoric irons with commercially utilized rebars, a thermo mechanically processed commercial rebar (TATA TISCON) was utilized in all the studies. The nominal composition of TATA TISCON as provided by the manufacturer was 0.17-0.24 C, 1.1 Mn, 0.05max S, 0.045max P, and 0.001max N. This commercial rebar had been produced by the TEMPCORE process which results in a hard martensitic rim and a softer ferrito pearlitic inner core [24].

The electrochemical behavior of the samples was studied in a standard flat cell (EG & G, USA) in freely-aerated 3.5% NaCl solution of pH 7, 0.5 M Na_2SO_4 solution of pH 3 and pore solution of saturated $Ca(OH)_2$ solution of pH 12.5 (with different chloride content) using silver-silver chloride electrode (SCC) as reference. The samples were polished up to 800 grade silicon carbide paper and degreased with acetone and finaly washed with distilled water before each

experiment. Tafel polarization and potentiodynamic polarization studies were performed in 0.5 M Na_2SO_4 and 3.5% NaCl using a scan rate 0.166 mVs^{-1} solution using a computer controlled potentiostat (PARSTAT 2263, EG & G, USA). In case of potentiodynamic polarization studies in pore solution with different chloride concentrations of 0.0, 0.05 and 0.1 %, a scan rate 0.5 mVs^{-1} was used. All the experiments were repeated three to four times.

Elechtrochemical impedance spectroscopy (EIS) studies were conducted using specially designed cells. This cell consiststs of a cylindrical flask (dia of 8.5 cm and height of 11.5 cm) with a cover on top, which had provisions in the form of circular openings of different sizes to permit the introduction of various electrodes. The solutions used for testing was saturated $Ca(OH)_2$ solution with different concentration (0.0, 0.05, 0.1 %) of chloride ions. EIS was performed after 1, 24, 48, 72, 96, 120 and 144 hrs using PARSTAT 2263 potentiostat by applying a sinusoidal potential perturbation of 10 mV at the open circuit potentials with frequency sweep from 100 kHz to 5 mHz.

The mechanical properties of the samples were also evaluated. Microhardness of each sample was obtained at least 15 times in a microhardness tester. Duplicate tensile tests were performed using cylindrical test specimens as per ASTM-A370 standard (diameter 4 mm and gauge length 16 mm). The tensile test pieces were strained at room temperature (27^0C) in a Hounsfield tensile machine (model H 20 K-W) of 20 kN capacity using a strain rate of 1.6×10^{-3} s^{-1}. This strain rate lies in the regime for 'static' tension test as defined by Dieter [17]. The fracture surfaces were examined in an FEI QUANTA 200 SEM using back scattered electrons.

3. .RESULTS AND DISCUSSION

3.1 MICROSTRUCTURAL CHARACTERISATION

The microstructures of the samples were obtained using two different etchants. In order to understand the etching action of Oberhoffer and 3% nital etchants, a region was provided an indentation using microhardness tester and this region was observed after etching with the two reagents. This is shown in Fig. 1(a) and (b). As copper (II) chloride is present in Oberhoffer reagent, copper precipitates on regions of low phosphorus. Therefore, in the optical microscope, the high phosphorus areas of prior ferrite appear light while low phosphorus (prior austenite) region appear dark [23]. Etching with nital revealed the unusual "ghosting" features within ferrite grains of samples B and sample C (Fig. 1(c) and (d)) [22]. From Fig. 1(b), it is clear that the light regions are of lower phosphorus content in the "ghost" microstructure. These samples (B and C) were forged between 1050^0C to 1100^0C in the dual phase region. As the transformation of austenite to ferrite is very slow in Fe-P alloys, the inhomogeneity of phosphorous content, between prior austenite and prior ferrite when the steels cool down from dual phase region to room temperature, remains. It even remains in case of very slow cooling [23]. "Ghost" lines mark the boundaries in phosphorus content arising from the dual phase ferrite-austenite microstructure. Nital preferentially attacks iron with lower phosphorus content, giving a surface relief that characterizes the phosphorus distribution [23]. It has been reported that the samples heat-treated from dual phase region showing "ghosting" with nital possess good mechanical properties in comparison to that forged below dual phase region [21]. Optical micrographs of samples B and sample C etched with Oberhoffer reagent are shown in Fig. 1(e) and (f). Sample C revealed lower inhomogeneity in P compared to sample B. In the regions showing no ghosting, the free phosphorus in solid solution may be low in case of sample C. The possible precipitation of of phosphide is anticipated because the Fe-P phase diagram [22] indicates that, beyond 0.1% P, phosphides can be precipitated. The microstructures of sample A (Fig.1(g)) did not reveal any inhomogeneity of phosphorus distribution. This is because sample A was hot forged in the gamma (austenite) region where phosphorus redistribution is not expected to take place. Therefore, after air cooling to room temperature, the austenite fully

converted to ferrite and there was no inhomogeneity of P distribution. Sample D revealed an outer martensitic rim and inner ferrito-pearlitic core, using nital etchant.

3.2 ELECTROCHEMICAL BEHAVIOR

The Tafel plots for all the samples in 0.5M Na_2SO_4 solution of pH 3 are presented in Fig. 2. The corrosion rates of the phosphoric irons were lower than that of reference sample. Moreover, the decrease in anodic currents for the Fe-P alloys should be noted. The stabilized free corrosion potential (E_{corr}) for samples A, B and C were found to be higher than the E_{corr} of mild steel (sample D) used as reference. This indicated that the phosphoric irons were noble compared to mild steel. The potentiodynamic polarization curves in 3.5 % NaCl solution (not shown here) provided similar results.

The potentiodynamic polarization plots in figure 3(a) were obtained in simulated pore solution of saturated $Ca(OH)_2$. Similar potentiodynamic polarization curves, obtained with saturated $Ca(OH)_2$ containing 0.05 wt. % chloride ions, indicated that the passive film on the samples was unaffected. The threshold value of chloride concentration for passive film breakdown was, therefore, higher than 0.05 wt.% for all the samples. In contrast to this, the potentiodynamic polarization curves in saturated $Ca(OH)_2$ with 0.1 % chloride (figure 3(b)), indicated that the pitting potentials for samples A and B were higher (more than 100 mV) than that of reference sample D. Sample C also revealed higher passive film break down potential than that of sample D but lower than that of sample A and B. Therefore, the threshold value of chloride content to initiate pitting for sample D may be equal to or slightly greater than 0.05 % Cl ion. This result is in conformity with that of Moreno *et al* [6] for AISI 1010 carbon steel. The causes for improved corrosion resistance of phosphoric iron is under investigation. It could be due to the presence of phosphorus in phosphoric iron catalyzing protective passive film formation. The passive film nature appears to depend on the free phosphorus present in the alloy. The lower pitting potential for sample C than that of A and B may be due to low free phosphorus in sample C due to the possible precipitation of phosphide, which was indirectly indicated in the microstructural characterization study. The microstructure will be characterized in detail using transmission electron microscopy in future.

Elechtrochemical impedance spectroscopy (EIS) studies in pore solution of saturated $Ca(OH)_2$ after six days of immersion revealed higher oxide pore resistance for samples A, B and C compared to commercial steel bar sample D (Fig.4). The EIS data, provided as Nyquist plots in figure 4 (a), revealed that the radius of the first semicircle of sample C was not distinguishable from that of second semicircle at lower frequency end. In sample B this was slightly distinguishable while the time time constants are clearly distinguishable in sample A and D. Appropriate modelling of EIS data using equivalent circuits indicated that the pore resistance of sample C was greater than that for B, followed by A. The lowest pore resistance was obtained in case of reference sample D. In the case of saturated $Ca(OH)_2$ containing 0.1% chloride ions, the Nyquist plots (figure 4(b)) again revealed the relativley superior pitting resistance of the phosphoric irons when compared wth sample D.

The free corrosion potential of the samples were also recorded as a function of time duing the long-term immersion study for EIS. A continuous increase in the difference between the corrosion potential in saturated $Ca(OH)_2$ and that containing 0.1% chloride ions was noticed with immersion time. The corrosion potentials shifting towards active values in the solution contining chloride ions. This change in corrosion potential towards active values was much higher in case of reference sample D than the phosphoric irons. The potential fall is due to acidification caused by pitting of chloride ions [25]. Visually, the surface of sample D was very severely damaged by pitting compared to the phosphoric irons. This is in confimity with the the

higher oxide pore resistance obtained for phosphoric irons. The EIS study confirmed the benefits of applying phosphoric irons for concrete reinforcement applications.

3.1 MECHANICAL BEHAVIOR

The engineering stress-strain curves of the samples are presented in figure 5(a) while the microhardness data, in figure 5(b). With increasing phosphorus content from 0.11 to 0.49 %, the yield stress (YS), ultimate tensile stress (UTS) and hardness increased, while the elongation and percentage reduction in cross-section area at failure decreased (Table 1). Sample A and B revealed good ductility whereas sample C fractured at UTS without necking. The relatively higher YS and UTS for sample C compared to sample B indirectly indicates the possible precipitation of phosphide in C. The mechanical properties for sample B were comparable with that of commercial reinforcing concrete bar. Microhardness of all the samples were in similar order as ultimate tensile stress (UTS) obtained from tensile testing. The variation of microhardness (the mean deviation) for reference sample D was found to be more than other sample (Table 1). This is because the outer marteniste rim revealed higher hardness than the inner ferrito-pearlitic core. The tensile specimen of the reference sample D was machined from a 16 mm dia rebar. Only the ductile ferrito-pearlitic matrix was incorporated in the tensile sample gauge length. Had the outer martensitic rim been present in case of commercial rebar, its ductility would have been still lower.

Typical fractographs are provided in figure 6. Sample A and D revealed ductile plastic failure (dimples of cup and cone morphology). In sample B, the failure mode was mixed, i.e. brittle-cleavage rupture with some dimple rupture. The fracture surface of sample C mainly revealed cleavage facets. Microvoids were not observed on fracture surface of sample C like those seen in other samples. From the point of view of ductility and strength, sample B revealed almost comparable properties to commercial rebar.

4. CONCLUSIONS

The possible use of phosphoric iron for concrete reinforcement application has been studied. Three phosphoric irons of composition Fe-0.11P-0.028C, Fe-0.32P-0.028C and Fe-0.49P-0.028C were evaluated, and compared to that of commercial mild steel rebar with respect to mechanical and electrochemical behavior. The salient conclusions of the study are:

1. Inhomogeneity of phosphorus distribution was observed with Nital and Oberhoffer's etchant. The segregation of P to grain boundary region was avoided by forging in the two phase region.
2. The mechanical properties of Fe-0.32P-0.028C was comparable with commercial mild steel rebar.
3. Polarization studies in several different electrolytes indicated that the phosphoric irons were more corrosion resistance than mild steel.
4. The threshold value of chloride content to initiate corrosion in concrete was higher in case of phosphoric irons than mild steel, based on electrochemical testing in simulated pore solution. The phosphoric irons were also more resistanct to pitting when compared to mild steel.
5. EIS studies in pore solution of saturated $Ca(OH)_2$ revealed the superior nature of passive film that formed on the phosphoric iron.

5. REFERENCES

1. S.D. Cramer, Jr. B.S. Covino, S.J. Bullard, G.R. Holcomb, J.H. Russell, M. Ziomlek-Moroz, Y.P. Virmani, J.T. Butler, F.J. Nelson and N.G. Thompson, *ISIJ International;* 42, (2002) 1376-1385.
2. S. Ahmad; *Cement and Concrete Composites*, 25 (2003) 459-471.
3. O. Poupard, A. Mokhtar, P. Dumargue and P. Dumargue, *Cement and Concrete Research*, 34 (2004), 991-1000.
4. T. Soylev and R. Francois, *Cement and Concrete Research*, 33 (2003) 1407-1415.
5.C. Alonso, C. Adrade, M. Castellote and P. Castro, *Cement and Concrete Research*, 30 (2000), 1047-1055.
6. M. Moreno, W. Morris, M. G. Alvarez and G. S. Duffo, *Corrosion Science*, 46 (2004), 2681-2699
7. S. C. Kuiry, S. Jha and A. Ganguly, *Trans. Indian Institute of Metals*; 53 (2000) 63-69.
8. R. Balasubramaniam and A.V. Ramesh Kumar, Corros. Sci. 42 (2000) 2085.
9. R. Balasubramaniam and A.V. Ramesh Kumar, Corrosion Science 45 (2003) 2451–2465
10. Gouthama and R. Balasubrmaniam, *Bull. Mater. Sci.*, 26, 2003, 483–491.
11. R. Balasubramaniam, *Current Science*, 85, 2003, 9
12. M. Yamashita, T. Misawa, Corros. Eng. 49 (2) (2000) 159
13. B. Clarke and I. Mcivor, *Ironmaking Steel* 16 (1989), 335-344
14. N. Allen, in Iron and its dilute solid solutions, (ed C. W. Spencer and F.E. Werner), Willey Interscience, New York, (1963), 271-308.
15. Y. Wang and C. Mcmahon, *Material Science Tenchnology,* 3 (1987), 207-216.
16. M. Goodway and R. M. Fisher, *His. Metal,* 22 (1988), 21-23.
17. G. E. Dieter, *Mechanical Metallurgy*, SI Metric Edition, McGrawHill Nework, (1988) 295-297 and 478-485.
18. H. Boyer and T. H. Tipler, *Journal of The Iron and Steel Institute,* 188 (1958), 218-237.
19. B. Hopkin, H. R. Tipler,", *Journal of The Iron and Steel Institute,* 188 (1958), 218-237.
20. S. Suzuki, M. Obata, K. Abiko and H. Kimura, *Transactions ISIJ,* 25 (1985), 62-68.
21. J.W. Stewart, J.A. Charles, and E. R. Wallach, 16, 2000, 275-282.
22. O. Kubaschewski, *Iron—Binary phase diagrams,* Berlin: Springer Verlag, (1982), 84–86
23. J.W. Stewart, J.A. Charles, and E. R. Wallach, *Material Science and Technology*; 16, 2000, 275-282.
24. B. Panigrahi and S. Jain, *Bulletin of Material Science,* 25, 2002, 319-324
25. P. Schiessl, *Corrosion of Steel in concrete*, Report of the Technical Committee 60-CSC RILEM (The International Union of Testing and Research Laboratories for materials and Structures), Chapman and Hall, London, (1988)), 57-62.

TABLE

Table-1 Tensile properties obtained from the engineering stress-strain curves.

Properties / Samples	YS (MPa)	UTS (MPa)	%Elongation (measured)	%Elongation from graph	% Reduction in Area	Average Hrdness (VHN) with std. devn
A	296	400	35	44	82	139 ± 9
B	365	504	31	47	67	202 ± 17.6
C	500	626	9	18	8	217 ± 18
D	340	448	34	47	79	201 ± 27

FIGURES

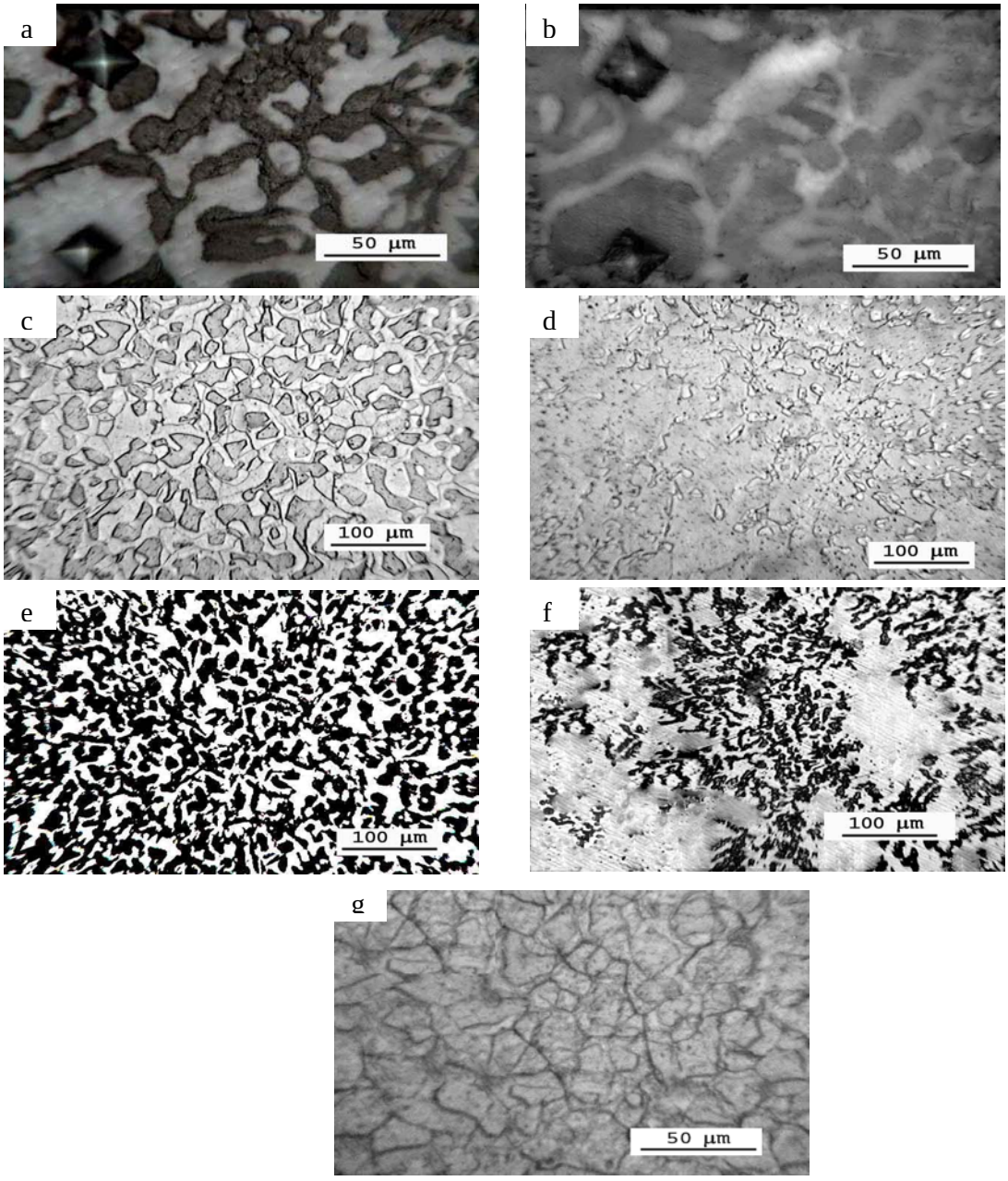

Fig. 1: (a) Sample B etched with Oberhoffer reagent, (b) Sample B etched with nital. This location is the same as that shown in Fig. (a), (c) Sample B etched with nital (d) Sample C etched with nital, (e) Sample B etched with Oberhoffer reagent, (f) Sample C etched with Oberhoffer reagent, (g) Sample A etched with nital

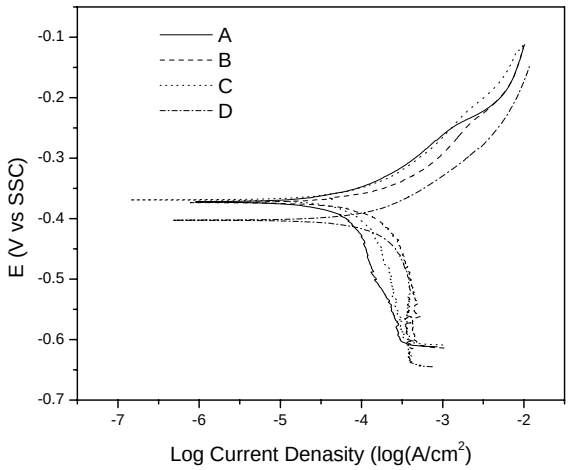

Fig. 2: Tafel plots for the alloys used in the study in 1 N Na_2SO_4 solution of pH = 3 obtained using a scan rate of 0.166mV s^{-1}.

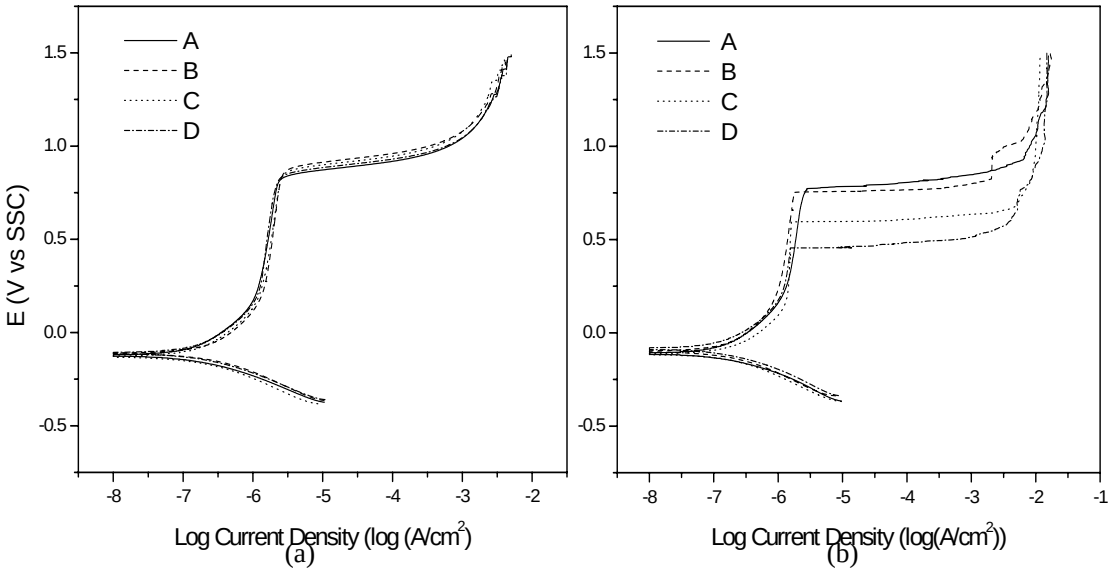

Fig. 3: (a) Potentiodynamic polarization curves in saturated $Ca(OH)_2$ solution of pH = 12.5 using a scan rate = 0.5mV/ s, (b) Potentiodynamic polarization curves in saturated $Ca(OH)_2$ solution of pH = 12.5 containing 0.1 % by wt. chloride ions

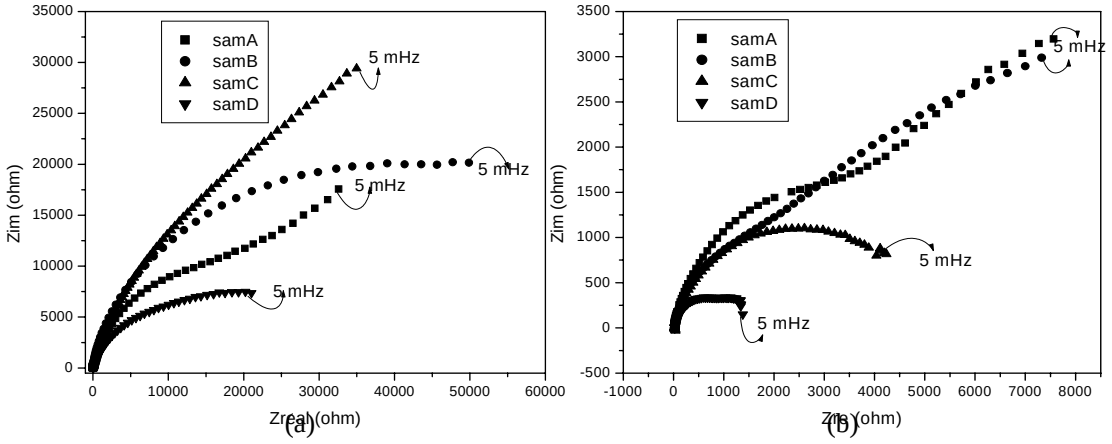

Fig. 4: Nyquist plots after 6 days of immersion in saturated $Ca(OH)_2$ (a) without chloride ion and (b) with 0.1 % chloride ions.

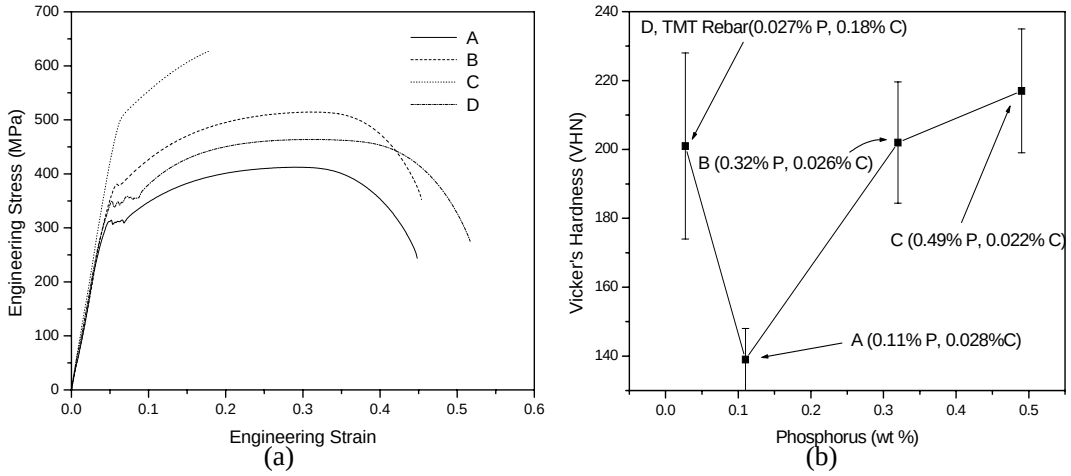

Fig. 5: (a) Engineering stress strain curves, and (b) variation of microhardenss as a function of phosphorus content.

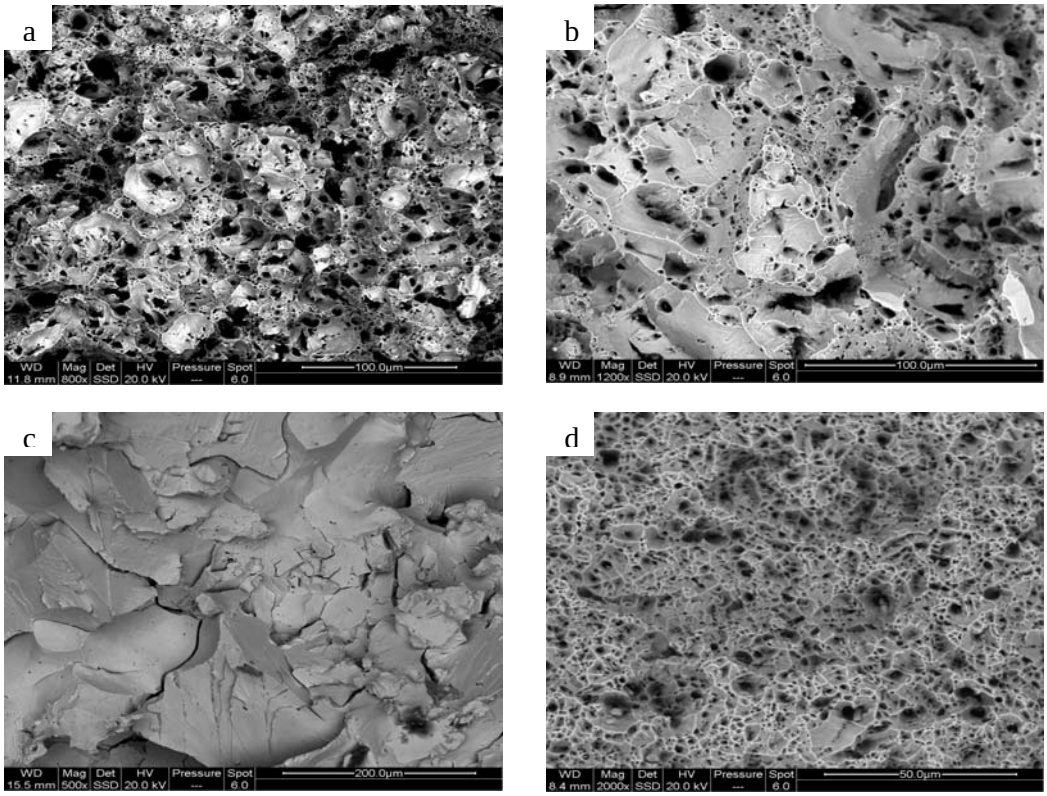

Fig. 6 SEM photographs of fractured surface of sample (a) A, (b) B, (c) C, and (d) D